Pergamon

Tetrahedron 56 (2000) 10081–10085

TETRAHEDRON

Structure Elucidation of Fumagillin-Related Natural Products

Judit Halász, Benjamin Podányi,* Lelle Vasvári-Debreczy, Anna Szabó, Félix Hajdú, Zsolt Böcskei, Judit Hegedűs-Vajda, Andrea Győrbíró and István Hermecz

Chinoin Co. Ltd. (a member of the Sanofi-Synthelabo Group)., Tó u. 1-5, H-1045 Budapest, Hungary

Received 27 July 2000; revised 27 September 2000; accepted 12 October 2000

Abstract—Fumagillin is currently the only means of treatment of microsporidiosis, which is frequent and fatal in AIDS patients. Results relating to NMR and X-ray crystallographic studies of fumagillin and the structure elucidation of three related compounds are reported. In the main impurity of fumagillin there is an exocyclic double bond instead of the spiroepoxide moiety. The solid-state and solution structures of fumagillin were compared with the conformation of fumagillin complexed to aminopeptidase-2.

Introduction

The structure of fumagillin (**1**) (Fig. 1) was deduced from X-ray investigation of a derivative of its hydrolysis product fumagillol.[1] It is a weak antibacterial agent,[2] but has a strong antiparasitic and amebicidal activity.[3] It has acquired importance in veterinary medicine, against microsporidiosis of bee and fish,[4] and in human medicine, against keratoconjunctivitis due to the encephalitozoon hellem.[5] Fumagillin was recently shown to cure severe intestinal infections of humans caused by microsporidia and cryptosporidia;[6] the latter caused a significant number of deaths among immunocompromised people during the water crisis in Milwaukee in 1993.[7] Fumagillin is currently the only treatment against cryptosporidiosis[6] and against microsporidiosis caused by the enterocytozoon bieneusi,[6] which are frequent and fatal in AIDS patients. The anticancer activity of fumagillin has long been recognized,[8] but the compound cannot be utilized because of its toxic side-effects. As a potent angiogenesis inhibitor, fumagillin suppresses the growth of a wide variety of tumors.[9] Derivatives with less side-effects have been synthesized, and one of them is now undergoing clinical trials.[10]

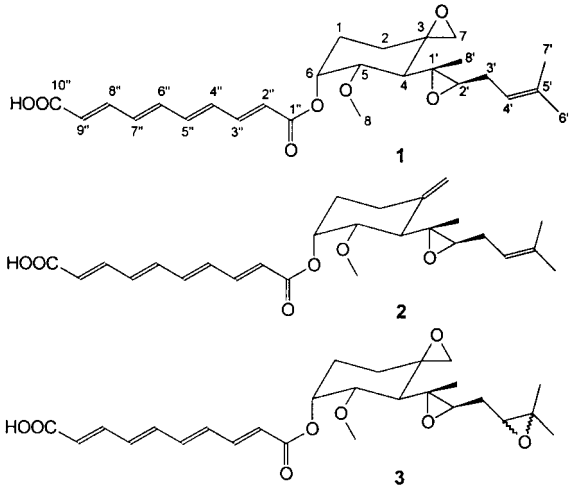

Figure 1. Fumagillin and its impurities.

Before the human application of fumagillin, the side-products formed during its fermentation should be identified. This demands the NMR spectroscopic and X-ray characterization of fumagillin. We report here results of NMR and X-ray crystallographic studies of fumagillin, and the structure elucidation of three related compounds.

Results and Discussion

X-Ray structure of fumagillin (1)

The single crystal X-ray study results (Fig. 2) reveal that the oxygen of the spiroepoxide ring is quasi-axial, the C-4 substituent and the methoxy group on C-5 are in the equatorial position, the decatetraenedioyl side chain is axial, and all four conjugated double bonds have the *E* configuration. The relative configuration of C-1′ and C-2′ to C-4 have also been determined and correspond to the expected structure.

NMR investigation of fumagillin (1)

Assignment of the NMR spectra. The protons of the

Keywords: conformation; X-ray diffraction; NMR; antiparasitic activity; amebicidal activity.

* Corresponding author. Tel.: +361-369-2500/2538; fax: +361-370-5597; e-mail: benjamin.podanyi@sanofi-synthelabo.com

0040–4020/00/$ - see front matter
PII: S0040-4020(00)00979-0

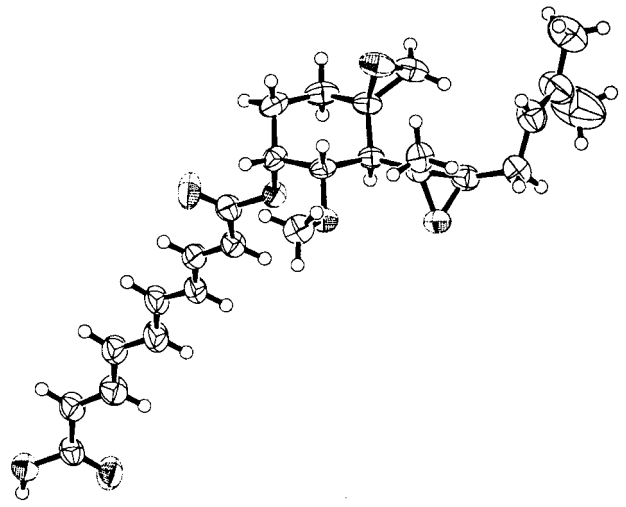

Figure 2. The structure of fumagillin.

cyclohexyl ring are denoted α or β, indicating their positions below or above the reference plane of the cyclohexyl ring (Fig. 3). The ^{1}H and ^{13}C signal assignments (Table 1) are based on COSY, HMQC[11], HMBC[12] and selective 1D TOCSY[13] measurements. 7-H_a and 7-H_b were assigned via the spatial proximity between 2-H_β and 7-H_a [from a NOESY[14] experiment].

Determination of proton–proton coupling constants. The proton–proton coupling constants of the aliphatic moiety of the molecule were determined by a first-order approximation from the ^{1}H NMR spectrum after Gaussian apodization for resolution enhancement. In the ^{1}H NMR spectrum the 4-H, 2-H_α and 3′-H_a signals overlap; the coupling constants of 2-H_α and 3′-H_a were obtained from selective 1D TOCSY spectra (Fig. 4). In the case of 2-H_α, the 2-H_β signal was excited selectively, and during the mixing time the magnetization passed through 2-H_β and 1-H_2 to 6-H, in giving the above-mentioned proton signals in the spectrum. Excitation of 4′-H resulted in the appearance of all of the protons of its spin system.

The spin system of the four conjugated double bonds is higher order, only the $^3J_{2'',3''}$ and $^3J_{8'',9''}$ coupling constants could be obtained by the first order approach. The vicinal coupling constants $J_{3'',4''}$, $J_{4'',5''}$, $J_{5'',6''}$ and $J_{6'',7''}$ were determined by means of spectrum simulation, which was performed with the PANIC program (Bruker) [$^3J_{HC=CH}$=15.2 Hz; $^3J_{HC-CH}$=11.2 Hz]. The coupling constant value $^3J_{HC=CH}$=15.2 Hz indicates the all-*E* configuration of the four double bonds in solution, in agreement with the X-ray data on the crystal.

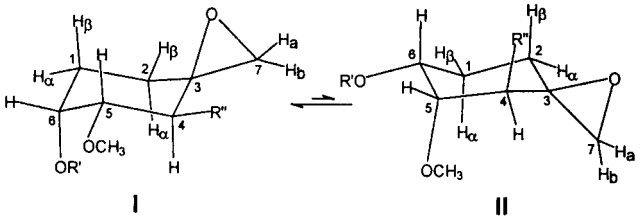

Figure 3. The two stable conformers of the cyclohexyl ring of fumagillin.

Investigation of the conformation of the cyclohexyl ring. Two stable conformers of the six-membered ring may exist, which were denoted **I** and **II** (Fig. 3).

The values $J_{2\alpha,1\beta}$=13.8 Hz and $J_{5,4}$=11.3 Hz suggest the diaxial arrangement of 2-H_α, 1-H_β and 5-H, 4-H. The coupling constants for conformer **I** were calculated from the molecular geometry obtained by the molecular mechanic calculation (MM^+ force field) using the modified

Table 1. ^{1}H and ^{13}C chemical shifts of **1**–**3** and proton relaxation times T_1 of **1**

	^{1}H			^{13}C		
	1[a,b]	**2**[b]	**3**[b,c]	**1**	**2**	**3**[c]
1 α	1.99 (0.36)	2.02	1.97	25.7	28.3	25.64 (25.56)
β	1.87 (0.35)	1.55	1.88 (1.83)			
2 α	2.12 (0.83)[d]	2.17[e]	2.10	29.4	30.3	29.2
β	1.09 (0.33)	2.30[e]	1.09			
3	–	–	–	59.5	145.2	59.5 (59.4)
4	2.08 (0.83)[d]	2.30	2.07	48.0	52.2	48.1 (47.9)
5	3.70 (0.72)	3.34	3.69	79.4	80.6	79.23 (79.19)
6	5.72 (0.77)	5.61	5.71	66.4	66.9	66.3
7 a	2.56 (0.49)	4.71	2.62	50.8	110.4	51.0 (50.9)
b	3.00 (0.47)	4.92	2.97			
8	3.45 (0.91)	3.43	3.43	56.7	56.6	56.6
1′	–	–	–	58.9	59.7	58.8 (58.5)
2′	2.68 (0.89)	2.71	2.85 (2.80)	61.0	61.3	58.9 (58.3)
3′ a	2.17 (0.83)[d]	2.26	1.76 (1.73)	27.3	27.6	28.3 (27.8)
b	2.39 (0.60)	2.40	1.76 (1.90)			
4′	5.21 (1.94)	5.22	2.93 (2.87)	118.7	118.9	61.4 (60.8)
5′	–	–	–	134.9	134.3	58.6 (58.3)
6′	1.75 (1.31)	1.73	1.32 (1.33)	25.7	25.7	24.59 (24.56)
7′	1.66 (2.02)	1.66	1.28 (1.31)	18.0	18.0	18.9 (18.7)
8	1.23 (0.78)	1.32	1.18 (1.23)	13.8	13.3	13.93 (13.87)
1″	–	–	–	166.1	166.2	166.0
2″	6.00 (1.89)	6.02	5.98	123.4	123.5	123.2
3″	7.29 (1.64)[f]	7.30	7.28	143.4	143.4	143.4
4″	6.44 (1.28)[g]	6.48	6.43	134.1	134.2	134
5″	6.59 (1.26)[h]	6.63	6.59	138.7	138.8	138.8
6″	6.59 (1.26)[h]	6.63	6.59	139.7	139.8	139.7
7″	6.46 (1.28)[g]	6.48	6.43	133.3	133.3	143.4
8″	7.33 (1.64)[f]	7.37	7.32	145.0	145.3	145.0
9″	5.94 (2.02)	5.97	5.92	122.3	122.0	122.2
10″	–	–	–	170.3	170.3	170.4

[a] Relaxation times T_1 [s] are given in brackets

[b] Coupling constants [Hz] of **1**: $J_{1\alpha,1\beta}$=14.3 Hz; $J_{1\alpha,2\alpha}$=4.3 Hz; $J_{1\alpha,2\beta}$=2.8 Hz; $J_{1\alpha,6}$=3.8 Hz; $J_{1\beta,2\alpha}$=13.8 Hz; $J_{1\beta,2\beta}$=4.4 Hz; $J_{1\beta,6}$=2.5 Hz; $J_{2\alpha,2\beta}$=13.8 Hz; $J_{4,5}$=11.3 Hz; $J_{5,6}$=2.8 Hz; $J_{7a,7b}$=4.4 Hz; $J_{2',3'a}$=6.9 Hz; $J_{2',3'b}$=5.9 Hz; $J_{3'a,3'b}$=14.8 Hz; $J_{3'a,4'}$=7.9 Hz; $J_{3'b,4'}$=6.9 Hz; $J_{3'b,7'}$=~1 Hz; $J_{4',6'}$=~1 Hz; $J_{4',7'}$=~1 Hz; $J_{2'',3''}$=$J_{4'',5''}$=$J_{6'',7''}$=$J_{8'',9''}$=15.2 Hz; $J_{3'',4''}$=$J_{5'',6''}$=$J_{7'',8''}$=11.2 Hz. Coupling constants [Hz] of **2**: $J_{1\alpha,6}$=4.6 Hz; $J_{1\beta,6}$=2.6 Hz; $J_{4,5}$=10.8 Hz; $J_{5,6}$=2.7 Hz; $J_{7a,7b}$=1.5 Hz; $J_{2',3'a}$=$J_{2',3'b}$=6.4 Hz; $J_{4',6'}$=~1 Hz; $J_{4',7'}$=~1 Hz; $J_{2'',3''}$=$J_{8'',9''}$=15.4; $J_{3'',4''}$=$J_{7'',8''}$=11.5 Hz. Coupling constants [Hz] of the major diastereomer of **3**: $J_{1\alpha,6}$=3.7 Hz; $J_{1\beta,6}$=2.8 Hz; $J_{4,5}$=11.2 Hz; $J_{5,6}$=2.8 Hz; $J_{7a,7b}$=4.2 Hz; $J_{2',3'}$=4.9,7.2 Hz; $J_{3',4'}$=4.4,7.9 Hz; $J_{4',6'}$=~1 Hz; $J_{4',7'}$=~1 Hz; $J_{2'',3''}$=$J_{8'',9''}$=15.4 Hz; $J_{3'',4''}$=$J_{7'',8''}$=11.4 Hz.

[c] The chemical shifts of the minor diastereomer are given in brackets; where no value for the minor compound is presented, the chemical shifts of the major and minor isomers were the same.

[d] The relaxation time could not be determined exactly because of signal overlapping.

[e] Tentative assignment.

[f] The relaxation time could not be determined exactly because of signal overlapping.

[g] The relaxation time could not be determined exactly because of signal overlapping.

[h] The relaxation time could not be determined exactly because of signal overlapping.

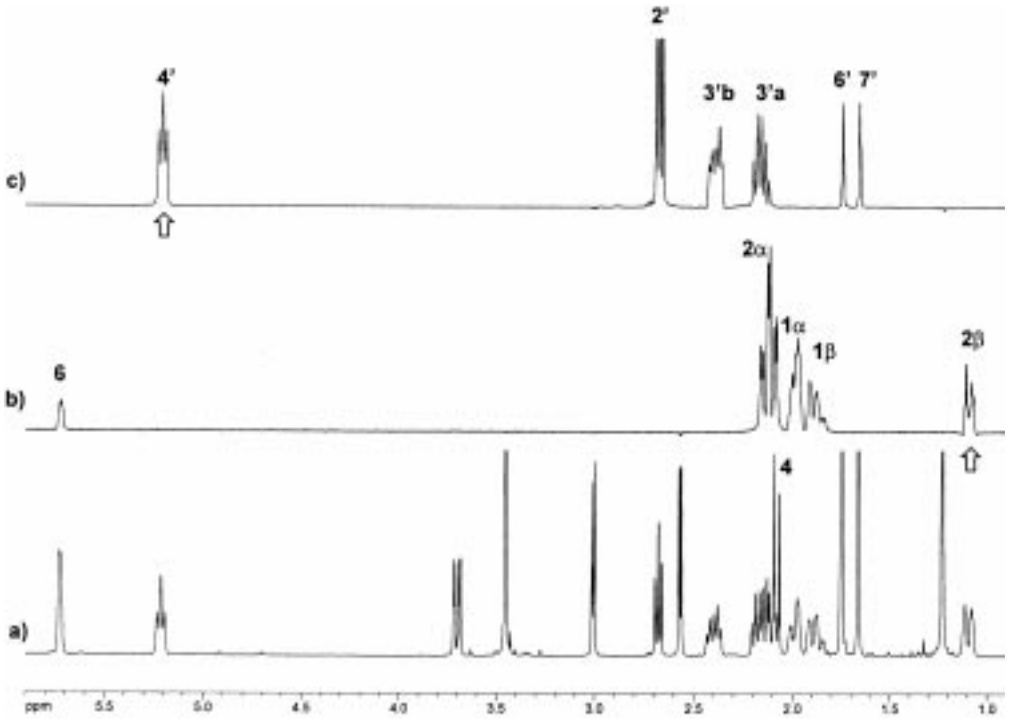

Figure 4. ^{1}H NMR (a) and selective 1D TOCSY (b,c) spectra of fumagillin.

Karplus equation.[15] The calculated [$J_{2\alpha,1\beta}$=13.7 Hz; $J_{5,4}$=12.0 Hz] and measured [$J_{2\alpha,1\beta}$=13.8 Hz; $J_{5,4}$=11.3 Hz] coupling constants are in good agreement, indicating that the population of conformer **II** in the conformational equilibrium is negligible beside that of conformer **I**.

The C-1″,6-H carbon–proton coupling constant was determined via a selective 2D INEPT[16] experiment (J=3.3 Hz). From the X-ray structure, the dihedral angle 6-H–C-6–O–C-1″ is 34°. From this value the $J_{C,H}$ coupling constant was calculated using the Karplus equation parametrized by Davies[17] for the C–O–C–H moiety. The calculated (J=3.8 Hz) and the measured (J=3.3 Hz) values are in good agreement, suggesting that the conformation around the C-6–O bond in solution is similar to that observed during the study of the single-crystal.

Conformational investigation of the C-4 side-chain. The vicinal proton–proton coupling constants of 3′-H_2 ($J_{2',3'a}$=6.9 Hz; $J_{3'a,4'}$=7.9 Hz and $J_{2',3'b}$=5.9 Hz; $J_{3'a,4'}$=6.9 Hz) seem to be averaged values, suggesting that no dominant conformer exists around the C-2′–C-3′ and C-3′–C-4′ bonds. The relaxation times of the hydrogens in the environment of the isolated double bond are longer than those in the aliphatic moiety of the molecule, again indicating greater flexibility in solution (Table 1). The increased anisotropic factors of C-6′ and C-7′ point to the increased dynamics of this moiety even in the solid state.

The spatial proximities 8′-H_3;5-H, 8′-H_3;7-H_b, 7-H_b;2′-H and 4-H;2′-H determined from the NOESY cross-peaks may be characteristic for the conformations along the C-4–C-1′ bond. The four distances given above were determined as functions of the dihedral angle 4-H–C-4–C-1′–C-2′ by means of MM. The expected NOESY volume integrals were calculated from the distances. The sum of the square of the difference between the calculated and measured volume integrals was plotted as a function of the dihedral angle (Fig. 5). The curve has a flat minimum between −10° and +30°. The 4-H;C-2′ dihedral angle is 44°. This suggests that in the dominant conformer(s) in solution the 4-H;C-2′ dihedral angle is somewhat different from that observed in the crystal. The C-8′,4-H carbon–proton coupling constant determined from a selective 2D INEPT experiment is 3.9 Hz. The coupling constant was calculated for the X-ray structure, for 4-H;C-2′ dihedral angles of 10° and 30°, giving 3.1, 5.2 and 4.3 Hz respectively. The calculation was performed via a newly parametrized Karplus equation,[18] where the effect of the epoxide ring on the coupling constant is taken into account as an oxygen substituent. The measured and calculated values are

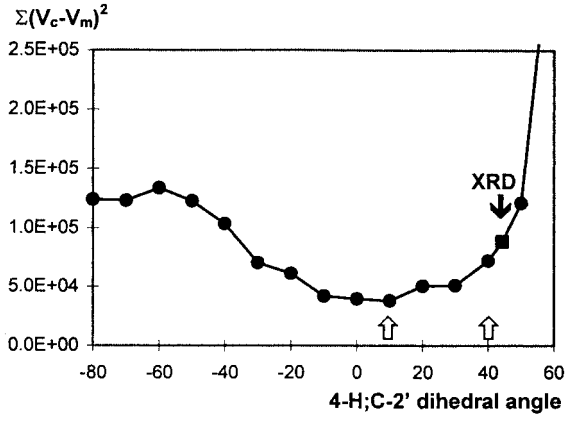

Figure 5. The volume integral differences as a function of the 4-H;C-2′ dihedral angle.

in good agreement at a 4-H;C-2′ dihedral angle of 30°, which supports the above reasoning.

Structure elucidation of fumagillin-related products (2 and 3)

The results of HPLC investigation revealed that the purchased fumagillin samples contained one related compound to an extent of 1.5–2% and several further compounds in significantly smaller amounts than that of the main impurity. To determine the structures of these related compounds, LC-MS measurements were performed. The main impurity eluting after fumagillin (at R_t=5.6 min) had a molecular mass of 442 D (16 mass units less than that of fumagillin). This compound was isolated by preparative HPLC. The high-resolution mass measurement on the quasi-molecular ion appearing at 442 D in the FAB+ spectrum indicated that the elemental composition of the impurity was $C_{26}H_{34}O_6$, i.e. one oxygen atom less than this number in fumagillin. The NMR (^{1}H, ^{13}C, DEPT-135, COSY, HMQC and HMBC) spectra proved that the main impurity (**2**) is similar to fumagillin, but contains an exocyclic double bond instead of the spiroepoxide ring (Fig. 1; Table 1). This impurity could not be removed from the fumagillin, so we attempted to decrease the amount of this compound by oxidation with *m*-chloro-perbenzoic acid. However, we observed that under such conditions fumagillin underwent oxidation to a mixture of two components in non-equal amount. The MS and NMR (^{1}H, ^{13}C, COSY, HMQC and HMBC) spectra demonstrated these corresponded to the two diastereomers of **3** (Table 1), the determination of the configuration of the newly formed epoxide moiety was not possible from the NMR data. Both isomers with similar ratio to the products obtained in the *m*-chloro-perbenzoic acid oxidation were found among the minor impurities of purchased fumagillin and they are degradation products formed during the study of stability of fumagillin.

Conclusion

The structure of fumagillin complexed to aminopeptidase-2 (MetAP-2) has been recently reported,[19] indicating that the inhibition of this enzyme is the reason for its antiproliferative activity.[10] We compared this structure with the conformations we obtained for fumagillin in the solid-state and in solution. The six-membered ring is in the same chair conformation (form **I**, Fig. 3) in all three structures. This conformation seems to be necessary for the antiangiogenic activity, since low activity was reported for a derivative of fumagillin where the other chair (form **II**, Fig. 3) is the dominant form of the six-membered ring.[20] The solution conformation around C-4–C-1′ (the proposed 4-H;C-2′ torsion angle of 30° corresponds to a C-2′;C-3 torsion angle of −89°) is in good agreement with the structure of fumagillin complexed to MetAP-2 (a C-2′;C-3 torsion angle of −87°), whereas it was slightly different in the crystal of fumagillin (a C-2′;C-3 torsion angle of −75°). The conformation around C-6–O, determining the position of the olefinic side-chain, is different in the enzyme-bound fumagillin (a C-1″;C-1 torsion angle of −135°) from that in the free form (a C-1″;C-1 torsion angle of −87°). This side-chain does not seem to be important from the aspect of activity, since several derivatives containing various side-chains were found to be good angiogenesis inhibitors.[9]

Three minor products were identified besides the fumagillin obtained by fermentation. The main impurity contains an exocyclic double bond instead of the spiroepoxide ring in fumagillin. A compound containing the same moiety was synthesized from biotin-fumagillin, and was reported to have a low antiangiogenesis activity,[21] since during the inhibition of MetAP-2 the spirocyclic epoxy carbon forms a covalent bond with an imidazole nitrogen of the enzyme. Further related products are the diastereomer pairs of the epoxide formed by oxidation of the isolated double bond of fumagillin, which were found to be degradation products during stability studies.

Experimental

The NMR spectra were recorded in $CDCl_3$ on a Bruker AVANCE DRX-400 NMR spectrometer, using standard Bruker software. Spectrum simulation was carried out with the PANIC program of the Aspect-2000 work station of the Bruker AC-200 NMR spectrometer.

Molecular modeling was performed with Hyperchem 4.0 (using MM^+ force field).

The MS measurements were made on VG TS-250 (EI+, FAB+), VG ZAB-2SEQ (FAB+) and LCQ (APCI+/−) equipment.

The LC-MS measurements were run on a Finnigan Mat LCQ instrument.

HPLC conditions for LC-MS measurements: Instrument: TSP R&D HPLC System; Stationary phase: Purospher RP18e, 125×3 mm; Mobile phase: acetonitrile/50 mM NH_4OAc (45:55); Flow rate: 0.6 ml/min; Detection: 348 nm.

2,4,6,8-Decatetraenedioic acid, mono[5-methoxy-4-[2-methyl-3-(3-methyl-2-butenyl) oxiranyl]-1-oxaspiro[2,5]-octan-6-yl]ester [3*R*-[3α,4α(2*R,3*R**),5β,6β(2*E*,4*E*,6*E*,8*E*)]] (1).** White powder, mp 192–194°C. $[\alpha]_D^{20}=-21.3°$ (c=1, EtOH–$CHCl_3$ 9:1), $[\alpha]_D^{20}=-27.3°$ (c=1, EtOH–CH_2Cl_2 4:1) [Found: C, 68.30; H, 7.36. $C_{26}H_{34}O_7$ requires C, 68.10; H, 7.47%]; ν_{max}(KBr pellet) 1712, 1630, 1447, 1372, 1276, 1233, 1161, 1015 cm^{-1}; *m/z* (EI): 459 (0.3, MH^+), 441 (0.1), 427 (0.1), 390 (1.5), 177 (48), 131 (59), 123 (53), 69 (100%); HRMS (FAB): MH^+, found 459.2364. $C_{26}H_{34}O_7$+H requires 459.2383.

Crystal data and structure refinement for 1. Empirical formula: $C_{26}H_{34}O_7$, Formula weight: 458.53, Crystal system: Monoclinic Space group: $P2_1$, Colorless, transparent, Unit cell dimensions: a=6.063(2) Å, b=13.6726(14) Å, c=15.6936(11) Å, β=92.641(13) deg. Temperature: 293(2) K, Z=2, Final R indices [$I>2\sigma(I)$]: R_1=0.0479, wR_2=0.1105, Goodness-of-fit on F2: 1.031 Crystallographic data for structure **1** have been deposited at the Cambridge Crystallographic Data Center (deposition number CCDC 149211).

2,4,6,8-Decatetraenedioic acid, mono[2-methoxy-4-methylene-3-[2-methyl-3-(3-methyl-2-butenyl)-2-oxiranyl]cyclohex-1-yl] ester [1*R*-[1β(2*E*,4*E*,6*E*,8*E*),2-β,3α(2*R,3*R**)]] (2).** The compound was isolated by a normal phase preparative HPLC. Instrument: NovaPrep 200 preparative HPLC system; Stationary phase: Nucleosil Si 100, 7 μm, 250 × 50 mm. Mobile phase: *n*-hexane/2-propanol/methanol/25% NH_4OH (770:130:100:3); Flow rate: 150.0 ml/min; Detection: 336 nm; Injection: 1 g (fumagillin)/150 ml. Fumagillin (1 g) was dissolved in 80 ml 2-propanol and then 70 ml of mobile phase was added to the solution. This solution was injected to the column. The fraction (5850 ml) was collected between 58 and 97 min retention time under argon atmosphere. Hexane was distilled off in vacuo (100 Hgmm) under nitrogen and the residual solution was evaporated to dryness in vacuo (10–15 Hgmm) under argon yielding 12 mg of yellowish oil. HRMS (FAB): MH^+, found 443.2425. $C_{26}H_{34}O_6+H$ requires 443.2434.

Diastereomeric mixture of 2,4,6,8-decatetraenedioic acid, mono[5-methoxy-4-[2-methyl-3-[2-(2,2-dimethyloxiranyl)ethyl]oxiranyl]-1-oxaspiro[2,5]octan-6-yl]ester [3*R*-[3α,4α(2*R,3*R**),5β,6β(2*E*,4*E*,6*E*,8*E*)]] (3).** To a stirred solution of Fumagillin (2.30 g, 5 mmol) in chloroform (20 ml) 3-chloroperoxybenzoic acid (0.95 g, 5,5 mmol) in chloroform (20 ml) was added dropwise at 5–10°C over a period of 30 min. After stirring for 2 h below 10°C the solvent was evaporated in vacuo at 20°C. To the residue 50 ml diethyl ether was added. The crystals were filtered off, washed with diethyl ether and dried in vacuo at room temperature. 2.15 g white crystals (yield: 90.6%) were obtained as a 7:3 diastereomeric mixture of **3**, mp 177–179°C. Recrystallization of the product from acetonitrile (30 ml) yielded 1.5 g of 3:1 diastereomeric mixture of **3**, mp 183–184°C. [Found: C, 65.61; H, 7.10. $C_{26}H_{34}O_8$ requires C, 65.81; H, 7.22%]; ν_{max}(KBr pellet) 1712, 1623, 1443, 1375, 1277, 1228, 1160, 1017 cm^{-1}; *m/z* (EI): 474 (0.4, M^+), 456 (1.4), 371 (0.5), 327 (1.2), 317 (0.9), 281 (0.8), 249 (2.4), 231 (4.0), 177 (43), 149 (18), 131 (58), 123 (50), 71 (100%).

References

1. McCorkindale, N. J.; Sime, J. G. *Proc. Chem. Soc.* **1961**, 331–331.
2. Hanson, T. E. *Antibiot. Chemother. (Washington DC)* **1951**, *1*, 54.
3. McCowen, M. C.; Callender, M. E.; Lawlis, J. F. *Science* **1951**, *113*, 102; Killough, J. H.; Magill, G. B.; Smith, R. C. *Science* **1952**, *115*, 71.
4. Girardeau, Jr., J. H. *Environ. Entomol.* **1972**, *1*, 519-520; Takeda Chemical Industries Jpn. Patent 43 204, 1982; *Chem. Abstr.* **1983**, *98*, 46950.
5. Diesenhouse, M. C.; Wilson, L. A.; Corrent, G. F.; Visvesvara, G. S.; Grossniklaus, H. E.; Bryan, R. T. *Am. J. Opthalmol.* **1993**, *115*, 293–298.
6. Molina, J. M.; Derouin, F.; PCT. Int. Appl. WO 9630010, CA., 125, 309073.
7. Hoxie, N. J.; Davis, J. P.; Vergeront, J. M.; Nashold, R. D.; Blair, K. A. *Am. J. Public Health* **1997**, *87*, 2032–2035; Rose, J. B. *Annu. Rev. Public Health* **1997**, *18*, 135–161.
8. DiPaolo, J. A.; Tarbell, D. S.; Moore, G. E. *Antibiot. Annu.* **1958–59**, 541.
9. Ingber, D.; Fujita, T.; Kishimoto, S.; Sudo, K.; Kanamaru, T.; Brem, H.; Folkman, J. *Nature* **1990**, *348*, 555–557.
10. Sin, N.; Meng, L.; Wang, M. Q. W.; Wen, J. J.; Bornmann, W. G.; Crews, C. M. *Proc. Natl. Acad. Sci.* **1997**, *94*, 6099–6103.
11. Bax, A.; Griffey, R. H. *J. Magn. Reson.* **1983**, *55*, 301–315; Bax, A.; Subramanian, S. *J. Magn. Reson.* **1986**, *67*, 565–569.
12. Bax, A.; Summers, M. F. *J. Am. Chem. Soc.* **1986**, *108*, 2093–2094.
13. Kessler, H.; Oschinat, H.; Griesinger, C.; Bermel, W. *J. Magn. Reson.* **1986**, *70*, 106–133.
14. Jeener, J.; Meier, B. H.; Bachmann, P.; Ernst, R. R. *J. Chem. Phys.* **1979**, *69*, 4546–4553; Wagner, G.; Wüthrich, K. *J. Mol. Biol.* **1982**, *155*, 347–366.
15. Haasnoot, C. A. G.; de Leeuw, F. A. A. M.; Altona, C. *Tetrahedron* **1980**, *36*, 2783–2792.
16. Jippo, T.; Kamo, O.; Nagayama, K. J. *J. Magn. Reson.* **1986**, *66*, 344–348.
17. Mulloy, B.; Frenkiel, T. A.; Davies, D. B. *Carbohydr. Res.* **1988**, *184*, 39–46.
18. Morvai, M.; Podányi, B. *Magn. Reson. Chem.* **2000**, *38*, 343–359.
19. Liu, S.; Widom, J.; Kemp, C. W.; Crews, C. M.; Clardy, J. *Science* **1998**, *282*, 1324–1327.
20. Marui, S.; Kishimoto, S. *Chem. Pharm. Bull.* **1992**, *40*, 575–579.
21. Griffith, E. C.; Su, Z.; Niwayama, S.; Ramsay, C. A.; Chang, Y. H.; Liu, J. O. *Proc. Natl. Acad. Sci.* **1998**, *95*, 15183–15188.